Proceedings, STESSA 2003, Behavior of Steel Structures in Seismic Areas, Naples, Italy, June 2003.

Component Testing and Modeling of Buckling Restrained "Unbonded" Braces

Cameron Black & Nicos Makris
Dept. of Civil Eng. & Envir. Engrg., University of California, Berkeley

Ian Aiken
Seismic Isolation Engineering, Inc., Oakland, CA

ABSTRACT: Following the behavior of building structures during recent earthquakes, it has been recognized that increased strength and stable energy dissipation capability are the most desirable mechanical characteristics needed to maintain interstory drift and overall displacements within tolerable levels. These requirements motivated the development of specially designed braces that can yield, yet not buckle. This paper presents test results from a comprehensive experimental program on such braces together with a mathematical model that approximates their hysteretic behavior.

1 INTRODUCTION

An early attempt to create a brace that dissipates energy yet does not buckle is reported in the paper by Kimura et al. (1976). The early seismic brace consists of a conventional brace encased in a square steel pipe filled with mortar. While Kimura et al. (1976) reported a few stable hysteretic characteristics it was found that following a compressive loading cycle that the transverse deformation of the mortar resulted in permanent void space large enough to allow local buckling during subsequent compressive loading. This concept was further refined by a team of investigators in Japan (Watanabe et al. 1988, Wada et al. 1989 among others) and resulted in what is known today as the *unbonded brace*™. The simplicity of its design and the outstanding performance of the *unbonded brace* has attracted the interest of industry and has been made commercially available by Nippon Steel Corporation.

Figure 1 presents a schematic showing the different components of the brace which merely consists of a steel core member encased in a steel tube filled with concrete. The steel core carries the axial load while the outer tube, via the concrete, provides lateral support to the core and prevents its global buckling. A thin layer of material along the steel core/concrete interface eliminates shear transfer during the elongation/contraction of the steel core and accommodates its lateral expansion when in compression. It is this ability of the core-member to contract and elongate free of frictional forces that these braces were given the name "Unbonded Braces".

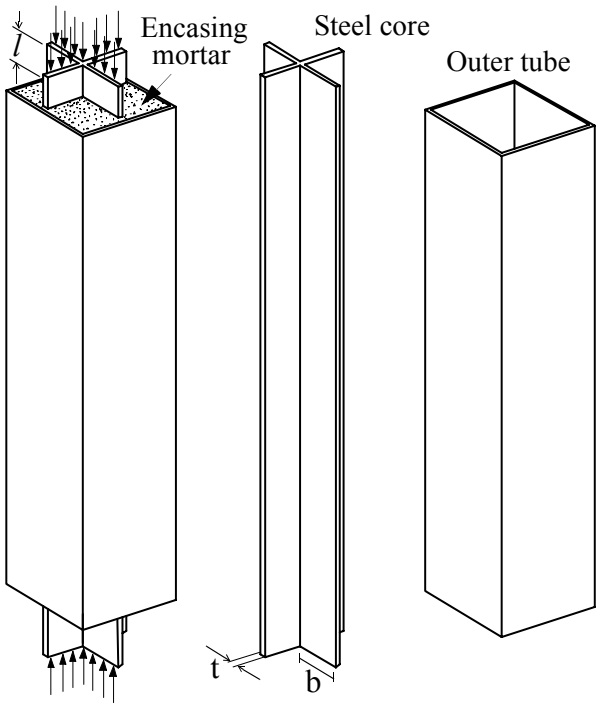

Figure 1. Schematic showing the different portions of the *unbonded brace*.

2 STABILITY ANALYSIS

The unbonded brace has three primary modes of instability: global buckling of the brace, buckling of the inner core in higher modes, and plastic torsional buckling of the portion of the brace which extends out from the steel tube.

The critical load at which the brace will buckle globally is given by the Euler buckling load

$$P_{cr} = \frac{\pi^2 E_o I_o}{L^2} \quad (1)$$

where E_o is Young's Modulus and I_o is the moment of inertia of the outer tube; while L is taken as the full end-to-end length of the brace.
The critical load for buckling of the inner core in higher modes is given by

$$P_{cr} = 2\sqrt{\beta E_t I_i} \quad (2)$$

where β is the distributed spring constant representing the stiffness of the encasing mortar, E_t is the tangent modulus, and I_i is the moment of inertia of the inner steel core. The value of the distributed spring constant, β, can be estimated be computing the one-dimensional compression modulus of concrete that is confined laterally by the presence of the steel tube and longitudinally by its neighboring concrete. Assuming plane strain conditions

$$\beta = E_c \frac{1-\nu}{(1+\nu)(1-2\nu)}. \quad (3)$$

For concrete material with a typical value of Young's modulus, $E_c = 21GPa$ and Poisson's Ratio, $\nu = 0.35$, $\beta = 33MPa \approx 4780ksi$. Wada et. al (1989) reported a comparable value of $\beta = 4480Ksi$. The critical load given by (2) is known to the literature (Timoshenko and Gere, 1961; Wada et al., 1989) and is independent of the boundary conditions of the brace (Black et al. 2002).

Another possible mode of buckling of the *unbonded brace* is the plastic torsional buckling of the portion of the inner core that protrudes from the steel tube/encasing mortar. The plastic buckling of a cruciform has been studied extensively in the literature, due in part to the fact that calculations based on the "less respectable" total deformation theory of plasticity correlated favorably with experimental data; whereas, the calculations from the more sophisticated incremental theory of plasticity departed appreciably from experimental results (Onat and Drucker 1952 among others). A recent study (Makris 2002) shows that if the flanges are slightly deflected the incremental theory of plasticity yields that the shear stress and shear strain at the onset of plastic torsional buckling are indeed related with the tangent shear modulus. The critical load from this study is

$$P_{cr} = \frac{A_i E_t}{3}\left[\frac{\pi^2}{3}\frac{b^2}{l^2} + 1 + 3\frac{\sigma_Y}{E_t}\right]\frac{t^2}{b^2} \quad (4)$$

where E_t is the tangent modulus, b is the width of the flange, l is the exposed length of the brace, σ_y is the yield stress, t is the plate thickness and A_i is the cross-sectional area of the section of the inner core that yields.

3 COMPONENT TESTING AT UC BERKELEY

The first experimental tests of the *unbonded brace* in the United States were conducted at UC Berkeley during the Spring of 1999 and Fall of 2000. This paper focuses on selected tests conducted in the Fall of 2000. Additional tests conducted by the same team of investigators can be found in a report by Black et al. (2002).

3.1 Test Setup and Loading Protocol

The test setup comprised two reaction frames anchored to the laboratory strong floor. A 700-kip hydraulic actuator with an in-line load cell was used for cyclic loading of the test specimens. The actuator had a displacement capacity of +/- 6 in., and was displacement-controlled via a linear variable displacement transducer mounted on the actuator. Figure 2 shows a view of the experimental setup for the Fall 2000 tests.

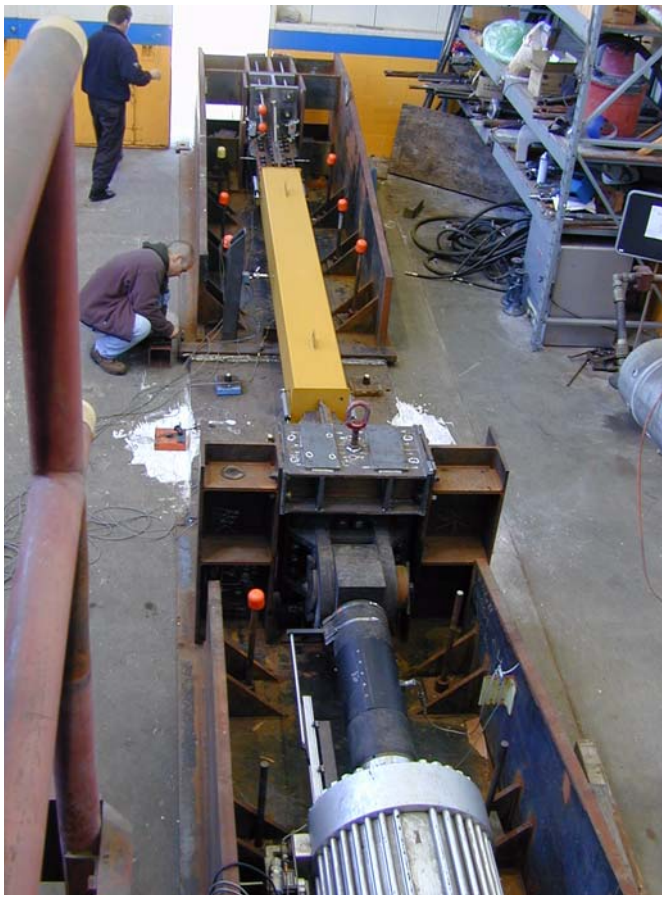

Figure 2. View of the experimental setup.

The test program for the braces consisted of two phases. First, each brace was subjected to a standard

loading protocol that was agreed on by the agency in charge of approving the use of the brace in the hospital—The Office of Statewide Health, Planning and Development (OSHPD). This brace loading history, referred to as the *OSHPD basic loading history,* was designed to subject the test specimens to maximum deformations and cumulative plastic deformations that exceeded the Upper Bound Earthquake (UBE) design demands. The primary parameter used to define the test program was the brace cyclic axial strain. The strain levels used correspond to building interstory drift ratios of 0.5, 1.0, 1.5, 2.0 and 2.25%. The test had 5 phases, each phase corresponding to 2 cycles at the prescribed strain level, for a total of 10 cycles. The *OSHPD basic loading history* tests were followed by additional tests including large-deformation, low-cycle fatigue tests and simulated earthquake displacement tests. The input motion for the upper-bound-earthquake tests was derived from a nonlinear analyses of an idealized, 5-story building enhanced with *unbonded braces* and subjected to the upper-bound-earthquake as defined by the code.

3.2 Brace Description

The two *unbonded braces* tested in fall 2000 are representative of the braces designed for the Kaiser Santa Clara Medical Center. The specimens tested had identical cruciform core members of Japanese Industrial Standard (JIS) grade SN400B steel with $34.1\ ksi \le \sigma_y \le 51.5\ ksi$. The tube steel was JIS STKR400. The end connection designs for the test specimens were consistent with those designed for the buildings. The bolts were 1-inch diameter, ASTM grade A490 and the splice plates were JIS grade SM490A steel which is approximately equivalent to ASTM A572/50. A summary of the brace properties is given in Table 1. Figure 3 shows the critical load for each of the buckling modes presented in the previous section and compares them to the axial yield load of the specimen. The maximum load on the brace during the design upper-bound-earthquake loading test is also presented. It is seen that the most critical mode is the plastic torsional buckling which has a factor of safety of 1.25 in comparison to the maximum load in the upper-bound-earthquake test.

3.3 Experimental Results

Figure 4 (top) plots the imposed end displacement of the *OSHPD basic loading history* and the corresponding measured force-displacement loops for specimen 00-12. The recorded hysteresis loops are full, nearly symmetric and stable. The force-displacement loops resulting from the low-cycle fatigue test performed on specimen 00-11 are shown in Figure 4 (bottom). The brace exhibited stable hysteretic behavior for the entire test consisting of 31 cycles. The initial intention was to conduct the test to failure which was anticipated to occur at approximately 20 cycles. This value was exceeded and subsequently the test was stopped at 31 cycles (without failure) in order to avoid potential damage to the instrumentation or test setup.

Table 1. *Unbonded braces* tested at UC Berkeley in Fall 2000.

Inner Core					
Specimen	Cross section type and dimension mm (in)	Area mm^2 (in^2)	Yield Length mm (in)	Steel Grade and yield stress MPa (ksi)	Py KN (kips)
00-11 00-12	(+) 19 x 197 (3/4 x 7-3/4)	7,125 (11.4)	3,410 (134.3)	JIS SN400B 285.4 (41.1)	2,033 (457.1)

Outer Tube				
Specimen	Cross section mm (in)	Buck-ling Length mm (in)	Steel Grade and yield stress MPa (ksi)	$P_{cr} = P_e$ pinned end KN (kips)
00-11 00-12	300 x 300 x 6 (9.8 x 9.8 x 0.24)	4,500 (177.2)	JIS STKR400 317.2 (46)	9911 (2228)

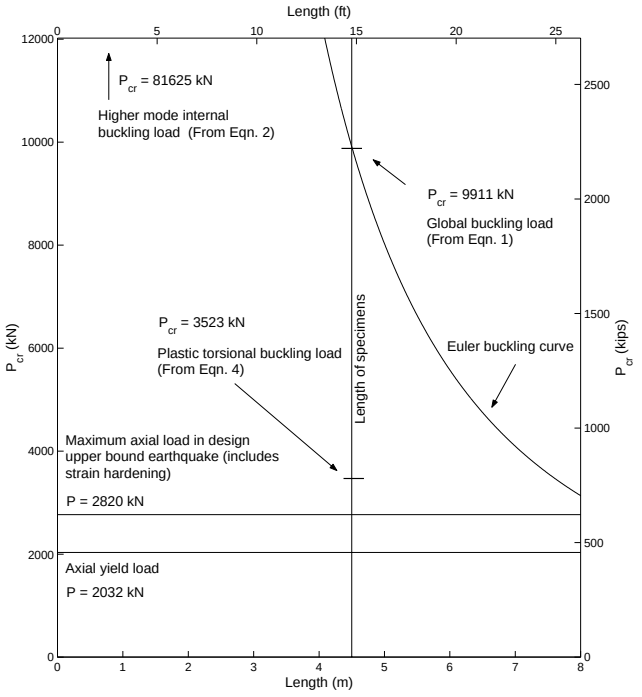

Figure 3. Plot showing the critical loads for global buckling, higher mode internal buckling and plastic torsional buckling for the specimens tested in comparison to the axial yield force of the brace. The plastic torsional buckling is seen to have the lowest margin of safety.

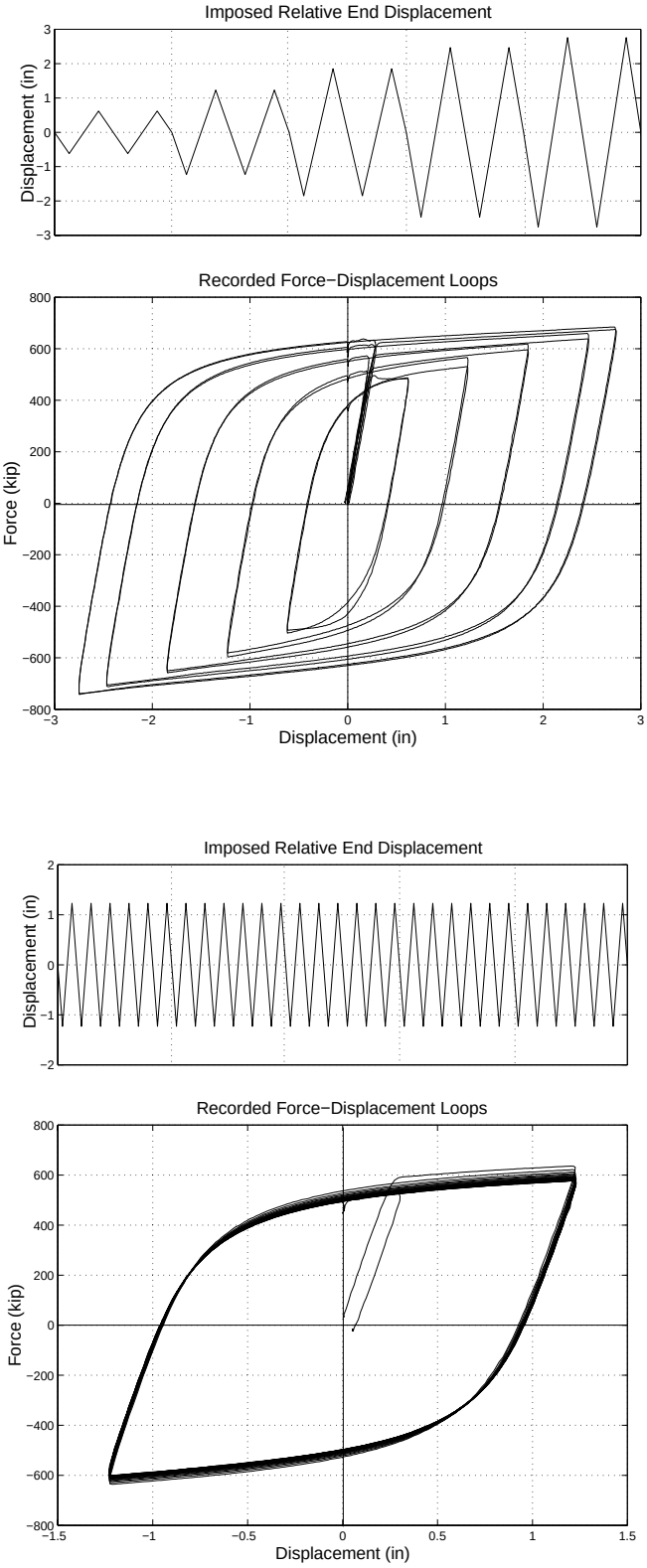

Figure 4. Plots showing imposed displacement histories and resulting force-displacement loops for the basic loading history performed on specimen 00-12 (top) and the low-cycle fatigue test performed on specimen 00-11 (bottom).

4 MODELING OF THE UNBONDED BRACE

A suitable model to approximate the nonlinear hysteretic behavior of the *unbonded brace* is given by

$$P(t) = \varepsilon K u(t) + (1-\varepsilon) K u_y Z(t) \qquad (5)$$

where $u(t)$ is the extension of the brace, K is the pre-yielding stiffness, ε is the ratio of the post- to pre-yielding stiffness, u_y is the yield displacement, σ_y is the yield stress of the core member, and $Z(t)$ is a hysteretic dimensionless quantity governed by the equation:

$$u_y \dot{Z}(t) + \gamma |\dot{u}(t)| Z(t) |Z(t)|^{n-1} + \beta \dot{u}(t) |Z(t)|^n - \dot{u}(t) = 0 . \qquad (6)$$

In the above equation β, γ, and n are dimensionless quantities that control the shape of the hysteretic loop. The hysteretic model, expressed by (5) and (6), was originally proposed by Bouc (1971) for n=1, subsequently extended by Wen (1975,1976), and used in random vibration studies of inelastic systems.

Figure 5 shows a comparison between the force-displacement loops obtained from the first phase (0.5% strain) of the *OSHPD basic loading history* for specimen 00-12 and those predicted by the Bouc-Wen model. The parameters K, ε and u_y can be estimated from brace geometry and material properties: $K = A_i E / L_i$, $\varepsilon = E_t / E$ and $u_y = \sigma_y L_i / E$, where A_i, L_i and σ_y are the area, length and yield stress of the yielding portion of the brace, E is the elastic Young's Modulus and E_t is the tangent modulus. Calibration therefore involves finding the values of β, γ, and n which best fit the experimental results. The values of β and γ are interrelated through the relation $\beta + \gamma = 1$, leaving two fitting parameters β and n (or γ and n) to be calibrated. The parameters used in Figure 5 are given in Table 2.

Table 2. Parameters used in Bouc-Wen Model

Parameter	Symbol	Value
Initial stiffness	K	2400 kips/in
Ratio of secondary to initial stiffness	ε	0.021
Yield displacement	u_y	0.19 in
Bouc-Wen parameter	β	0.55
Bouc-Wen parameter (1- β)	γ	0.45
Bouc-Wen parameter	n	1

The calibrated Bouc-Wen model is subsequently used to approximate the behavior of the brace when subjected to a seismic input. Figure 6 (top) shows the displacement history of the upper-bound-earthquake, while Figure 6 (bottom) shows the performance of the Bouc-Wen model in approximating the response of a brace to the upper-bound-earthquake. The solid line corresponds to data measured experimentally, whereas, the dashed line corresponds to the response predicted by the Bouc-Wen model for the same input

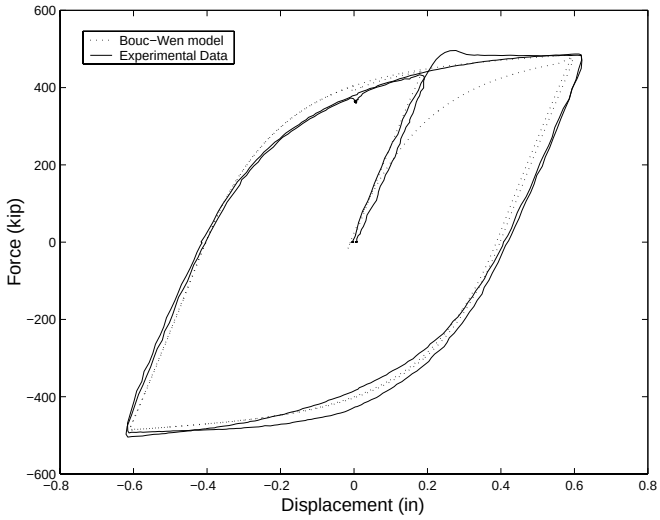

Figure 5. Comparison of Bouc-Wen model to experimental data collected during the first inelastic cycles.

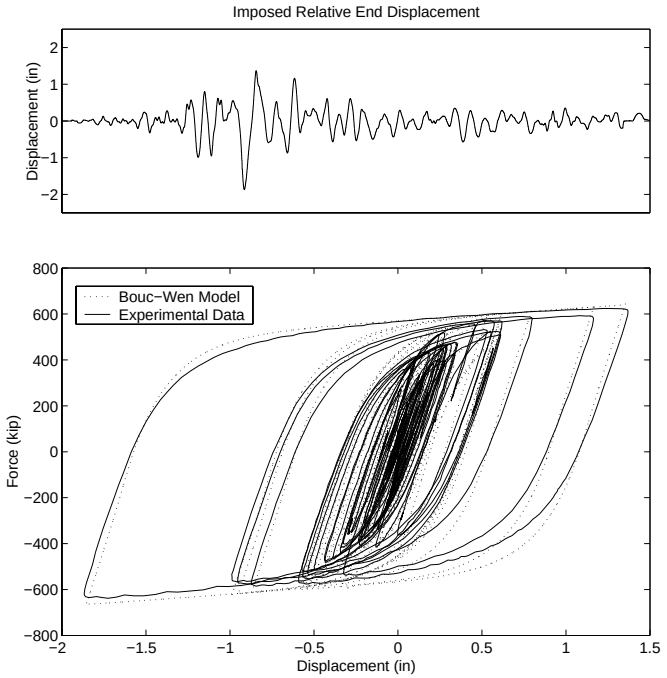

Figure 6. Plot showing the upper-bound-earthquake (top) and a comparison between the recorded force-displacement loops and those obtained from the Bouc-Wen model (bottom).

displacement. All parameters given in Table 2 remain the same except the yield displacement, u_y, which was increased to 0.24 in. (a 25% increase) to account for strain-hardening.

5 CONCLUSIONS

This paper summarized results from cyclic testing of *unbonded braces* at UC Berkeley. The braces, which are representative of the braces designed for use in the Kaiser Santa Clara Medical Center, demonstrated stable and repeatable behavior for all tests. Of the potential modes of instability discussed in this paper—including global buckling of the brace, higher mode internal buckling and plastic torsional buckling—it was found that the plastic torsional buckling of the inner core is the most critical mode with a factor of safety of 1.25 with respect to the maximum load induced in the brace during the design upper-bound-earthquake. The macroscopic behavior of the brace was modeled using the Bouc-Wen hysteretic model which was shown to match the experimental behavior with fidelity.

6 ACKNOWLEDGEMENTS

The unbonded braces and the financial support for their testing were provided by Nippon Steel Corporation, Japan. Technical assistance during testing in the Structural Research Laboratory at the Richmond Field Station, University of California, Berkeley was provided by Mr. Don Clyde, Mr. Wes Neighbour and Mr. David MacLam. Their help is greatly appreciated.

7 REFERENCES

Black, C. J., Makris, N. and Aiken, I. D. (2002). "Component testing, stability analysis and characterization of buckling restrained "unbonded" braces," *Technical Report PEER 2002/08*, Pacific Earthquake Engineering Research Center, U.C. Berkeley.

Bouc, R. 1971. "Modèl mathématique d'hysteresis," *Acustica* 24: 16-25.

Kimura, K., Takeda, Y., Yoshioka, K., Furuya, N. and Takemoto, Y. (1976). "An experimental study on braces encased in steel tube and mortar," Annual Meeting of the Architectural Institute of Japan (In Japanese).

Makris, N. (2002). "Plastic Torsional Buckling of a Cruciform Column," *J. of Engrg. Mech.* ASCE. In press.

Onat, E. T. and Drucker, D. C. (1952). "Inelastic instability and incremental theories of plasticity," *Journal of the Aeronotical Sciences*, Vol. 20, No. 3, 181-186.

Timoshenko, S. P. and Gere, J. M. (1961). *Theory of Elastic Stability*, McGraw-Hill, New York, NY.

Wada, A., Saeki, E., Takeuch, T., Watanabe, A. (1989). "Development of Unbonded Brace," *Column* (A Nippon Steel Publication), No.115 1989.12.

Watanabe, A., Hitomoi, Y., Saeki, E., Wada, A., Fujimoto, M., (1988). "Properties of Braced Encased in Buckling-Restraining Concrete and Steel Tube," *Proceedings of Ninth World Conference on Earthquake Engineering*, Tokyo-Kyoto, Japan, Vol.IV, pp.719-724.

Wen, Y-K. 1975. "Approximate method for nonlinear random vibration," *J. of Engrg. Mech.* 102(EM4): 389-401. ASCE.

Wen, Y-K. 1976. "Method for random vibration of hysteretic systems," *J. of Engrg. Mech.* 102(EM2): 249-63. ASCE.